Proceedings of OMAE2005
24th International Conference on Offshore Mechanics and Arctic Engineering (OMAE 2005)
June 12-16 2005 Halkidiki Greece

OMAE2005-67451

ENHANCEMENT OF DESIGN CRITERIA FOR FISH FARM FACILITIES INCLUDING OPERATIONS

Are Johan Berstad
Dr. Ing. Aquastructures www.aquastructures.no,
Email: are.berstad@aquastructures.no

Harald Tronstad
Dr. Ing. Aquastructures www.aquastructures.no,
Email: harald.tronstad@aquastructures.no

Stein-Arne Sivertsen
M. Sc. Aquastructures www.aquastructures.no,
Email: stein-arne.sivertsen@aquastructures.no

Endre Leite
M. Sc. Hydrotech group
Email: endre.leite@hydrotech.no

ABSTRACT
A Norwegian Standard NS 9415 (NAS, 2003) has been introduced to the offshore fish farming industry in Norway. This is the first standard dealing with offshore fish farm facilities. The main objective of the standard is to reduce environmental pollution by fish escape.

The work process leading to NS 9415 revealed the need for research work in several areas to enhance design criteria with the objective of having a consistent safety level through out the life cycle of a fish farm facility.
This paper presents results from a government supported research project with the objective of enhancing criteria for design and operation of fish farm facilities.

A case study of a fish farm facility representative for the majority of polyethylene based fish farms in Norway is presented and the sensitivity of such fish farms to variation in the mooring system is shown and discussed for design relevance. The sensitivity of net cage volume to current and weights is presented and discussed. Possible hazards from operational conditions are listed.

INTRODUCTION
As of April 1st 2004 a Norwegian Standard NS 9415 was introduced to the offshore fish farming industry in Norway. This was the first technical standard world wide to be applied for such facilities.

The standard, NS 9415 specify technical criteria fish farm facilities need to comply with in order to be acknowledged for use in Norway.

Origins for fish escape have traditionally been both design failures as well as operations on the facility. During the process of creating NS 9415 it was seen that there was a need for a research effort in order to obtain a consistent safety level for different criteria to be met in the standard as well as possibly enhance the scope of the rules to also include fish welfare and HMS in addition to fish escape.

As part of a joint industry effort, Aquastructures as a certification body within the industry have initiated a research project to establish operational conditions to be considered for design of such facilities as well as to enhance design criteria for the other limit states.

There have recent years been several research efforts on fish farm facilities. Fredheim and Faltinsen (2003) have proposed a model to calculate the response of net structures. In this model the wake behind meshes is derived and hence fluid velocities, making it possible to account for velocity reduction behind the mesh analytically. So far this has generally been based on empirical values (e.g Løland 1991). Lader et. al. (2003) use a time domain drag load approach similar to the present for waves and current, but have an alternative formulation for the net structure elements as well as for the drag and lift force. Fredriksson et al (2003) has compared calculations with measurements for a type of fish farm where a linearized approach was applicable allowing for them to carry out a frequency domain analysis.

Typical fish farm structures in the market today have too large deflections when exposed to wave and current forces that linearized approaches are not applicable in order to account for the highly flexible structures interacting with fluid forces in a hydroelastic manner. A typical such fish farm structure is shown in Figure 1

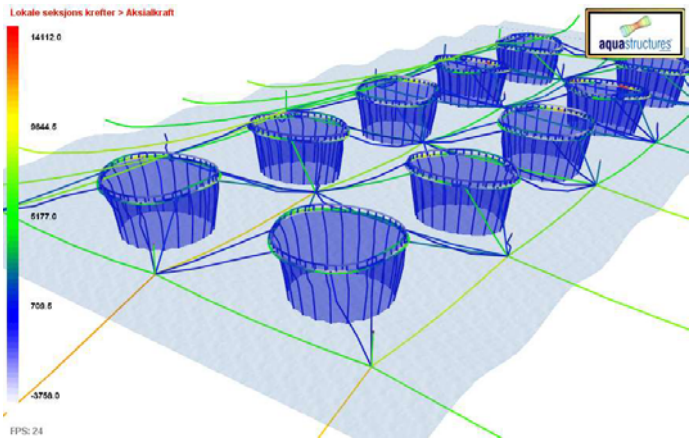

Figure 1 Typical fish farm facilities based on polyethylene floaters

The project presented in this paper deals with three major aspects:

- Operations on the fish farm facility involving the net structure.
- Use of weights or other means to hold the net volume.
- The influence of forces in the floaters by how the mooring system is established.

The project utilizes results and tools developed in an earlier project as described in Berstad et al (2004). In Berstad et al (2004) the numerical methods utilized in the numerical tool AquaSim is outlined and results from model testing has been compared to calculated results in a validation approach for the numerical tools used.

The work presented in this paper focus on some of the issues considered necessary to evaluate in order to revise of the standard, NS 9415 which will commence this year. A case study typical for a majority of existing aquaculture facilities based on polyethylene material in Norway is presented.

NOMENCLATURE

E = Young's modulus

$\Re^3$ = Cartesian 3D space

INTEGRATED FISH FARM SYSTEMS

Integrated fish farm systems are typically built up with a flag shaped fishnet with weights in the areas close to the bottom of the fish nets and a floater giving the buoyancy. A mooring system is attached to the floater. How the different components are attached together in a typical polyethylene cage system is shown in Figure 2.

Most commercial fish farms consist of several floaters as similar to the case seen in Figure 1. Systems with up to 20 and 30 cages exist. Typical systems based on steel cages may be seen in Berstad et al (2004).

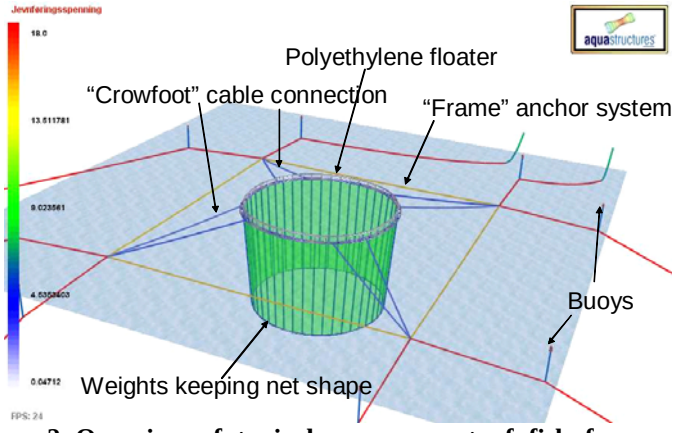

Figure 2 Overview of typical arrangement of fish farm facilities.

CASE STUDIES

The fish farm system seen in Figure 2 is used as the case study in this paper. Figure 3 shows in detail part of the floater. The vocabulary used in the paper is given in Figure 2 and Figure 3.

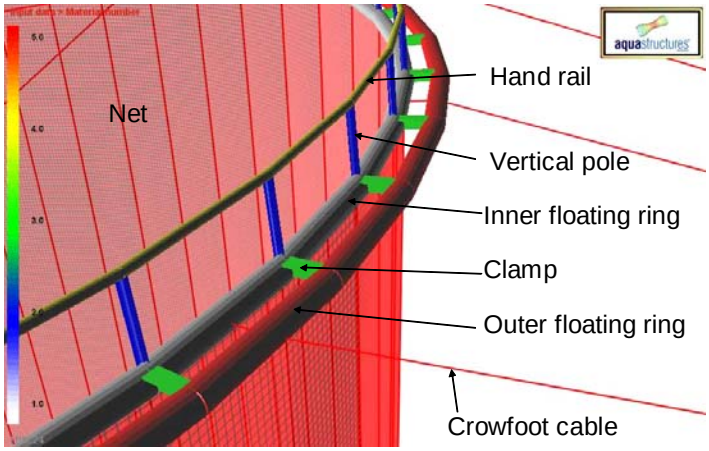

Figure 3 Detailed view of part of the floater structures

As seen from Figure 2 and Figure 3, the floater consists of two floating rings, handrail and 48 vertical poles and clamps. The net is attached to the inner floating ring. The distance between the inner and outer floating ring (centre to centre) is 0.6 m and the vertical distance between the inner floater to the handrail is 1.1 m. (centre-centre). The circumference of the inner ring is 90 m.

All the components in the floater are modeled with beam elements accounting for large geometric deformations (e.g. Halse, 1997). The floating rings are in general modeled with one element between consecutive clamps. The polyethylene pipes have a diameter of 315 mm and a thickness of 15 mm. Where the crowfoot is attached there are two elements between consecutive clamps. The crowfoot is attached to the outer ring as seen in Figure 3 and then through to the inner ring as seen in the figure. Hand rails are modeled with one element between consecutive frames. The vertical poles are modeled using one element. The polyethylene handrails and vertical poles have a diameter of 110 mm and a thickness of 9 mm. All floater components have a Young's module of 0.8 GPa and a Poisson's coefficient of 0.3. They all have a mass density of 950 kg/m^2. The clamps (also polyethylene) are modeled as T shaped cross sections with a cross sectional area of 1030 mm^2 and a sectional

modulus about the vertical and horizontal axis of 1.64E-6 mm^4 and 5.86E-6 mm^4 respectively. The clamp and the vertical pole are modeled such that they can slide along the horizontal tubes with a friction coefficient of 10%.

The water line is located 65 mm. above the bottom of the floaters at static equilibrium. Hydrodynamic forces are applied to the inner and outer floating ring at their actual position during simulation (see e.g. Berstad et al 2004)

Figure 4 shows key data for the mooring system. The system is symmetric about a vertical plane trough the centre point of the cage both in the vertical and horizontal direction as seen in Figure 4. All components in the mooring system are modeled with bar elements.

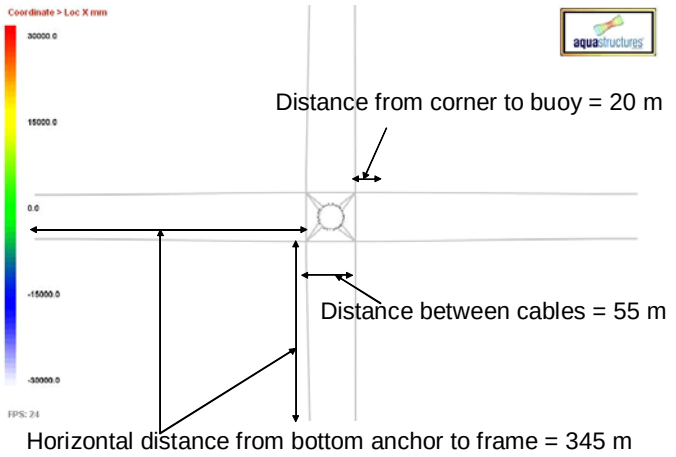

Figure 4 Key data for the mooring system

All mooring cables, except the section closest to the bottom, are standard polypropylene ropes with a diameter of 48 mm. The Young's module is 2GPa. Close to the bottom there is a 16.7 meters long steel cable with a diameter of 24 mm. The sea bottom is located at 100 m. The square frame part of the mooring system is located 5 meters below the surface. There are fully submerged floating devices at the corners with an upward force of 750 N. There are 8 linear surface piercing buoys having a water plane area of 0.3 m^2 and a submergence of 0.5 meters as modeled. The density of the polypropylene cables is set to 950. A relative weight in water of 3 N per meter is added.

The fish cage net is modeled with membrane elements. There is one element between each clamp, and 10 elements in the vertical direction. There are 48 vertical net staves which are modeled with bar elements. The vertical net staves have a Young's module of 2.0 GPa. Considering each twine of the net separately, the net itself has a Young's module of 1.0GPa. the diameter of each twine is 2 mm. The meshes are square and the length between knots is 20 mm. This gives a solidity of 0.2. The net is assumed to have no marine fouling on it. Both the net and the net staves are not assumed to have any relative weight in the water.

The net is 20 meters deep and the bottom of the net is not included in the computer model. The weight at the bottom of the net keeping the shape in waves and current is introduced by a filled polyethylene ring. As default this component has a relative weight in water of 1100 kg in total. The bottom ring is a 180 mm PE pipe with a thickness of 32 mm. The ring is modeled as a beam. The net is modeled slightly conical such that the circumference of the bottom ring is 81.7 meters.

The method used to carry out the time series simulations of the largely hydroelastic response is outlined in Berstad et al (2004).

For bar elements the Morison formulae is used with the cross flow principle (see. e.g. Faltinsen 1990). The load application to membranes is analogous to the Morison approach used for cables, but for membranes a lift component is accounted for. The present calculations follow the approach of Tronstad (2000).

A reduction coefficient r, is introduced for net structure or part of net structure located behind other net structures (See e.g. Løland 1991).

$$r=1.0 -0.46*Fac \quad (1)$$

where

$$Fac =0.04+(-0.04+0.33Sn+6.54S_n\text{^}2-4.88S_n\text{^}3)*\cos(alfa) \quad (2)$$

where S_n is the solidity of the net and alfa is zero if the current velocity is normal to the net.

When Morison loads are applied both the mass of the structure as well as added mass in the cross sectional plane is accounted for. Due to the large deflections occurring, the added mass is nonlinear.

The mooring cables have pretension as shown in Figure 5. Red color indicates an axial force in the cable of 4.4 kN. In the crowfoots the axial force is 350 N. For actual facilities in the industry this will vary strongly.

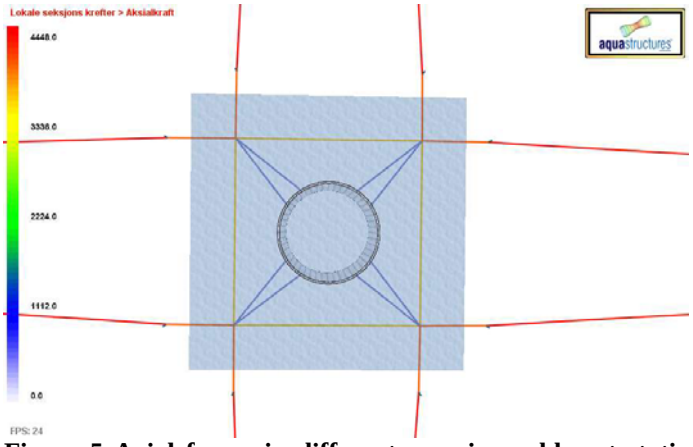

Figure 5 Axial forces in different mooring cables at static equilibrium

Figure 6 shows the vertical displacement of elements in the facility relative to the modeled positions. Red color means upward motion of approximately 1 meter and grey color means downward motion of approximately 6.5 meters. The steel chains close to the bottom are modeled horizontally.

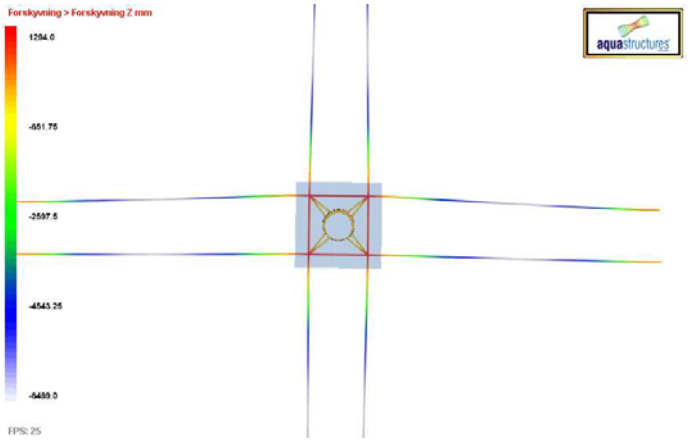

Figure 6 Vertical displacements at static equilibrium

The forces on the net structure from waves and current are the most important forces acting on the structure globally.

Case study 1 Stiffness variation in mooring

According to the governmental regulations enforced in Norway (NMF 2003) fish farm facilities may be certified as one full facility or alternatively the main components such as e.g. floater may be certified as components. A certification process requires documentation of the structural response of the given component in an idealized system. For a floater this means that the response of the floater is investigated for a given sea state in an idealized mooring system, such as the one shown in Figure 4. NS 9415 specify a range for the validity of this idealization. In the process of establishing the rules and regulations it was agreed that research was needed to investigate the sensitivity of forces in the floater as a function of mooring systems.

Consider the accidental load criteria of one mooring cable being cut. This accidental condition has to be fulfilled in order to meet NS 9415. Polyethylene fish farms have shown susceptible to this accidental load case. This is due to the skew response pattern. A similar skew response pattern will occur for cases where there is a difference in the length and hence stiffness for mooring cables. Figure 7 shows a response pattern for such a case. This will influence the distribution of forces in the mooring cables as well as in the floating rings strongly.

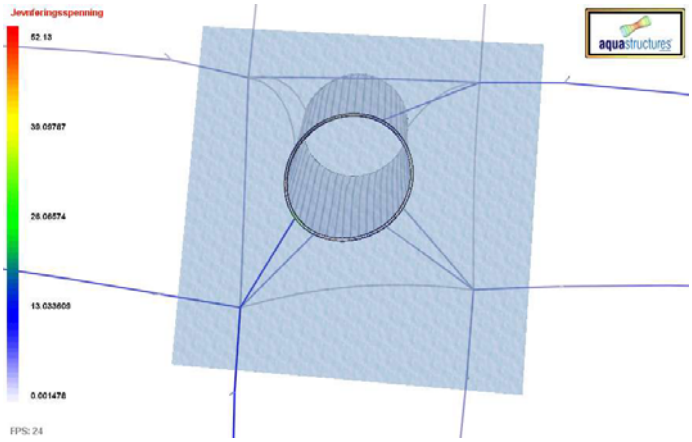

Figure 7 Deflection with skew mooring system

Consider a case where the lower left mooring line seen in Figure 7 from the buoy to the bottom has a young's modulus of 1.0E10. Then the Young's modulus of the right bottom cable in Figure 7 is varied from 1.0E03 to 1.0E10. All other values are as described earlier. The applied load in this case is a current velocity of 0.5 m/s with no waves.

Figure 8 shows the maximum force in the crowfoot cables as a function of varying the E-modulus of the right bottom mooring cable. As seen from the figure, the maximum forces in the crowfoot cables decrease as the stiffness of the lower right cable increase. The forces are lowest in case of symmetry (Log(10)E = 10) for both cables.

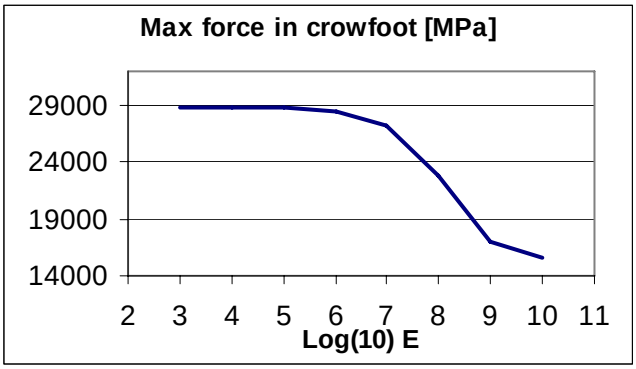

Figure 8 Maximum forces in crowfoot cable

As seen from Figure 8 the maximum forces in the crowfoots stabilize when the lower right cable softens. As seen from the figure, the value reaches an asymptotic value. The asymptotic value corresponds to the accidental limit state case of having a cut mooring cable.

Figure 9 shows maximum stress level in the floating rings at the same variation in mooring line stiffness as presented in Figure 8. As seen from this figure the maximum stress level is three times as large in the case with very skew response compared to the symmetric case. Comparing the results in Figure 9 and Figure 8, it is seen that the skewed mooring system is of even larger importance for the stress level in the floating rings than the forces in the crowfoot cables.

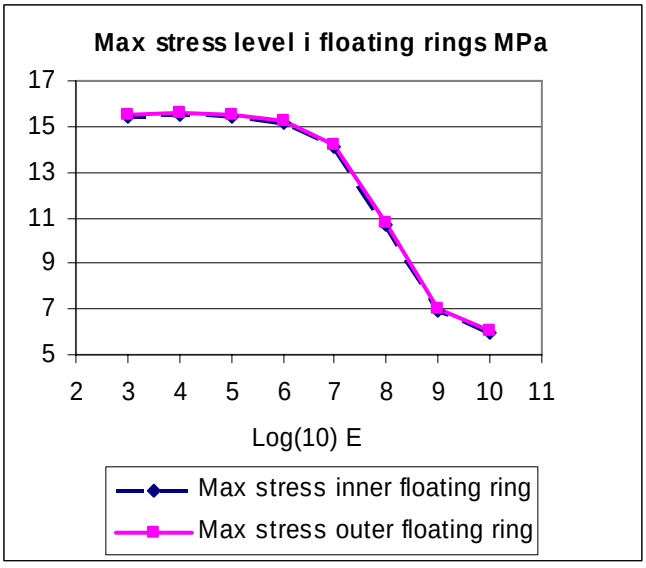

Figure 9 Maximum (principal) stress level in floater rings

There are many parameters influencing the sensitivity of stresses both in the mooring system and the floating rings

depending on the actual design of the fully integrated system. The results presented in this case study shows that the sensitivity to physical effects differs for different components in a system and there should be clear bounds as to what variations to allow without analyzing the fully integrated system. As seen from Figure 8 and Figure 9 a simplification that has been used by assuming proportionality between maximum crowfoot cable force and maximum ring stress level may underpredict the latter, in the case shown with approximately 50 %.

Case study 2 net volume in current and waves

Historically it has been experienced among marine fish farmers in Norway that mortality of the fish stock can be large in cases where the fish farm has been exposed to strong current or high seas, loss of more than half the stock has been experienced. One origin for the high mortality is the reduction in cage volume caused by the deflection of the net. This effect has not been included in the NS 9415 since only effects causing fish escape have been included thus far. It may however be included in a rule revision or it may be introduced to standards concerning fish welfare. A news article in Altaposten(2004) refers to a case during autumn 2004 where large fish death occurred due to volume compression in the net.

Deriving a methodology for calculating net volume in current and waves is included in the present research project. The following algorithm is proposed to calculate the volume of net cages with or without the bottom part:

Consider a typical net as shown in Figure 12. The vertical part of the net is modeled with membrane elements. At the top, an average node, p_i, is established by locating six boundary nodes in each direction of $\Re^3$ where the net is attached to the inner floater (giving a bounding box) and averaging these points.

$$(x,y,z)_{pi} = ((x_{max}\text{-}x_{min/})/2, (y_{max}\text{-}y_{min})/2, (z_{max}\text{-}z_{min})/2) \quad (3)$$

The above equation can be modified to alternative means of establishing a centre point. This leads to triangular plane elements having one side along the circumference and two lines from the circumference to point p_i. For this particular case this means 48 triangular elements as shown in Figure 10.

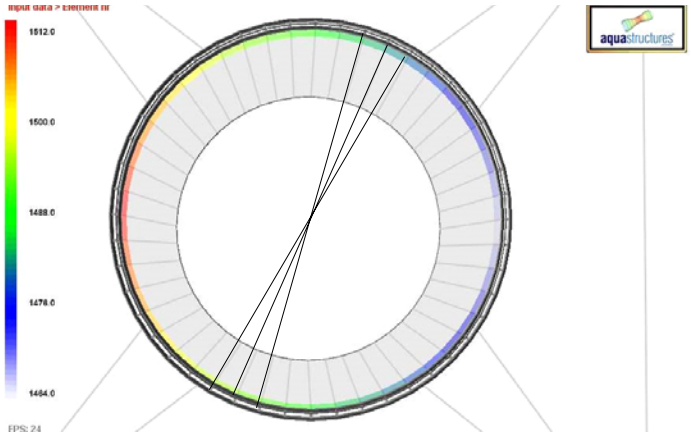

Figure 10. Artificially introduced triangular faces at the top of the net cage

The same algorithm is applied along the bottom edge of the net in case the bottom is not modeled. It is assured that the normal vector of all membrane elements points outwards. This result in a concave object in $\Re^3$ enclosed by a surface area made up by polygons of vertically quads for membranes, and triangular polygons artificially introduced at top and bottom to generate a closed object. Then, the divergence theorem is applied as in the approach of D. Eberly (1991) to convert the volume calculation into an area calculation.

$$\iiint_{\Omega} \nabla F dV = \iint_{S} F n dS \quad (5)$$

Given a differentiable vector field F, defined in a region Ω where n is the outer normal to the boundary of Ω, we approximate the boundary Ω with a Riemann sum over all quads and triangles we have in the computer model. This is seen in Figure 11. Choosing F = (x,y,z)/3, $\nabla F = 1$ and the volume integral becomes the volume of the region.

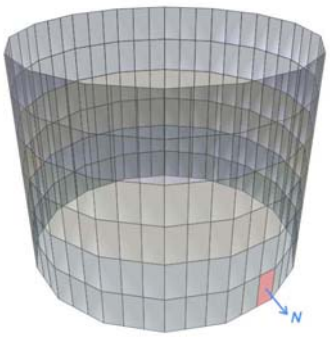

Figure 11. Approximation of surface contribution

The total volume is then approximately given by the equation (6) where $(x,y,z)_i$ is a point in the ith polygon plane, and $(u,v,w)_i$ is the normal vector illustrated in Figure 11.

$$V_{\Omega} = \sum_{i=1}^{m} (x_i u_i + y_i v_i + z_i w_i) \cdot \frac{1}{3} A_i \quad (6)$$

This algorithm is then applied at each time instant for a deformed mesh with updated element areas and normal vectors.

Figure 12 shows the deformed net with an applied current velocity of 0.2 m/s.

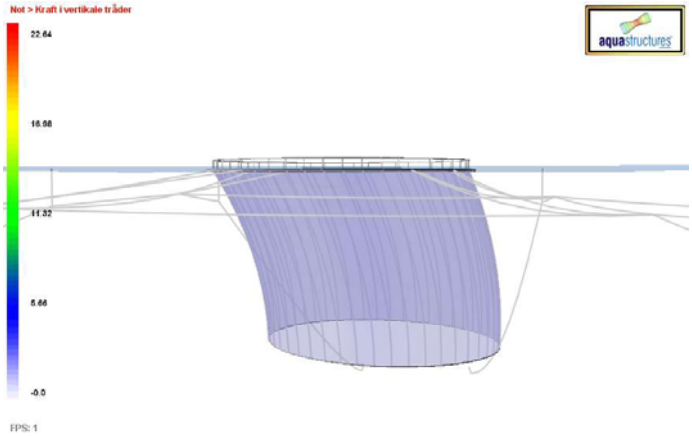

Figure 12 Case study fish net exposed to current with a velocity of 0.2 m/s

Figure 13 shows the deformed mesh with an applied current velocity of 0.6 m/s. As seen from this figure it is clear that the mesh volume is significantly reduced compared to the initial volume.

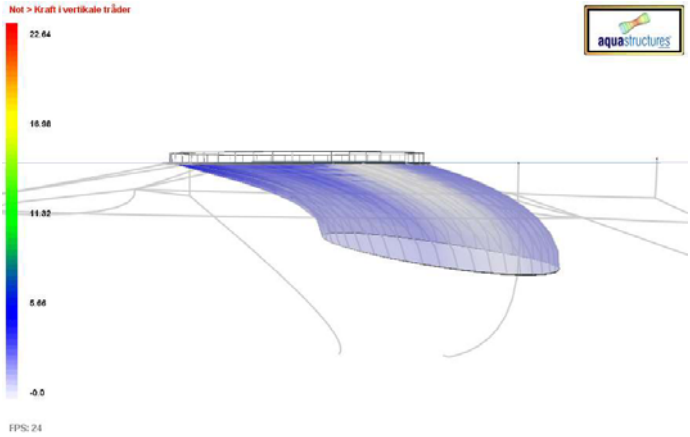

Figure 13 The case study fish net exposed to current with a velocity of 0.6 m/s

Figure 14 shows the deformed mesh with an applied current velocity of 1.5 m/s. As seen from this figure, the mesh volume very largely reduced for this large current velocity.

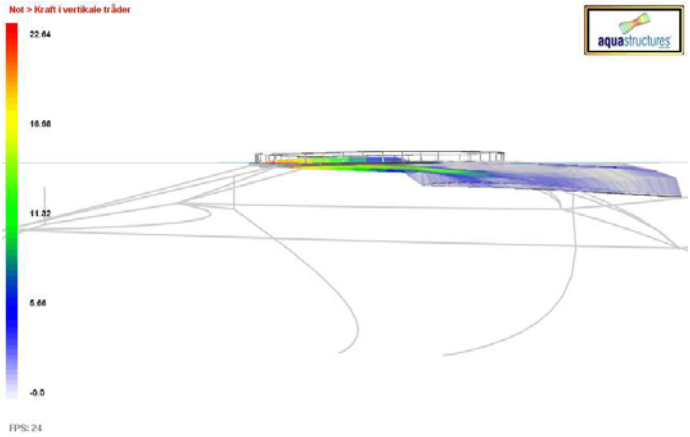

Figure 14 The case study fish net exposed to current with a velocity of 1.5 m/s

Figure 15 shows net volume as a function of current velocity. The solid line is for the case described above, where as the dashed line is for a case where everything is the same apart for the bottom ring being modeled as a bar, omitting the bending stiffness of the ring.

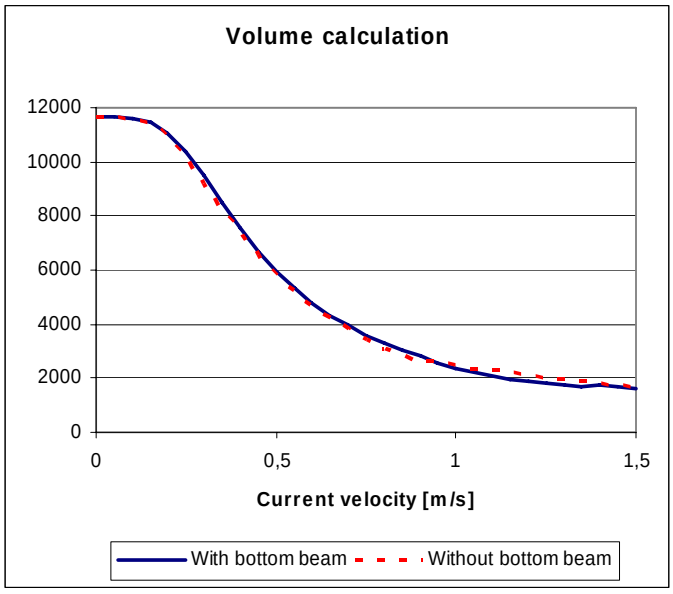

Figure 15 Net volume as a function of current velocity

As seen from Figure 15 the fish cage volume is significantly reduced as the current velocity increase. As seen from this figure the net volume is only half of the original value when the current velocity, U = 0.5 m/s. At U = 1.0 m/s, the volume is reduced to 20 % of the original volume, and at U = 1.5 m/s, the volume is 14 % of the original volume.

Net volume has also been considered by Lader and Enerhaug (1995) who reported a 35 % reduction of net volume in an experimental setup with a current velocity of 0.5 m/s. This setup can not be compared with the case study used in the present paper, but their relation curve between current velocity and volume shows a rather similar relation as seen in Figure 15.

As seen from Figure 15, the results differ slightly for the two considered cases with, and without, a bottom ring respectively. Figure 16 shows the difference in volume between the two models at each considered current velocity. The results are shown in terms of the volume at a time instant for the case with bending stiffness in the bottom ring divided by the same volume for the case without bottom ring. As seen from Figure 16, the volume there is a variation of approximately 10 % between the two cases. For low an intermediate current velocities, the net volume is larger when a ring is applied. This is plausible since the bottom ring will help spanning the net out at the bottom. However the volume is lower with ring at very large current velocities. At this stage however, the current is far too strong for any fish in the cage. As seen from Figure 16 the present calculations revealed only small differences between having a bottom ring or not. For certain cases nets have been reported (orally) to fold in a pattern leading to reduced volume if there is no bottom ring. This was not seen in the present case study, but should be looked further into.

The deformation of the net will change the flow pattern around the mesh such that there will be a decrease in oxygen exchange compared to a mesh with the original mesh shape. In

an undeformed mesh, stronger current will lead to more oxygen for fish. The large deformation may however give less oxygen for the fish. Hence not only the deformed volume may be of importance, but also the shape of the mesh.

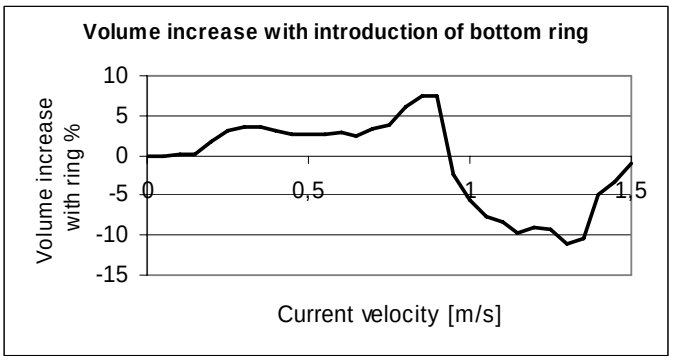

Figure 16 Difference in volume between two different models

The practical action a fish farmer may carry out to avoid reduced volume in the mesh due to current and waves is to increase the weights at the bottom of the net. Figure 17 shows the volume of the fish cage as a function of current velocity for cases where the bottom ring has a weight of 200, 1200 and 2400 kg respectively.

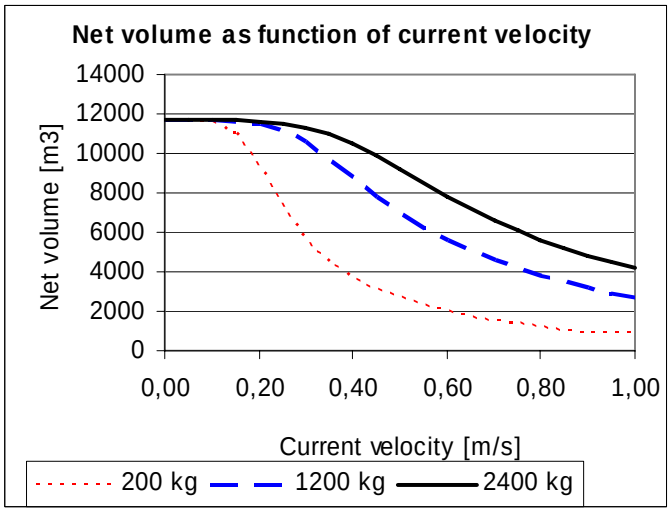

Figure 17 Net volume as function of current velocity

Figure 18 shows the net volume as function of bottom weight for current velocity 0.2 m/s, 0.5 m/s and 1.0 m/s.

As seen from Figure 17 and Figure 18 the net volume is strongly dependent on the bottom weights, and as expected more weights means more net volume in current. However increasing the weights also means more buoyancy or less freeboard. Less freeboard may violate demands for the accidental load condition of flooded compartment in NS 9415. This means in general that more weights means more cost for the fish farmer, but may in turn also generate more revenue if fish mortality is decreased during rough conditions.

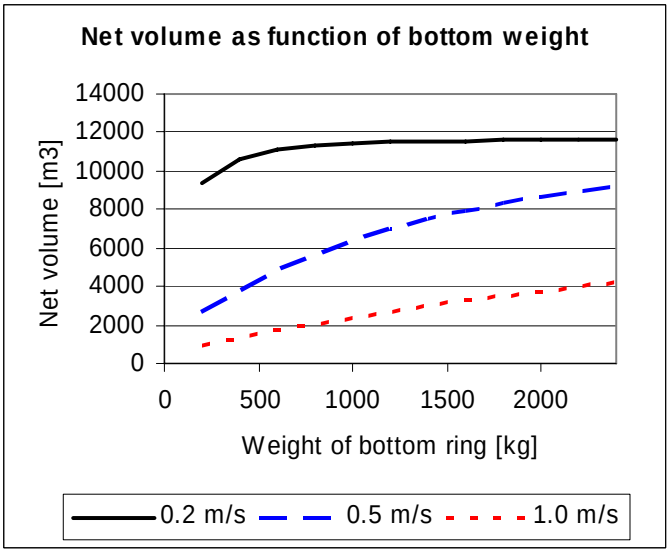

Figure 18 Net volume as function of bottom ring weight

Figure 19 shows the volume during a wave cycle with a wave height 3 meters and period 5.5 sec. The current velocity is 0.4 m/s. The first cycle is not a full wave, but the amplitude is built up during the cycle. As seen from the figure. The volume difference during a wave cycle is approximately 10 % for this particular case. A more comprehensive study on net volume in waves is recommended for further studies. Such study should include models both with and without the bottom part included as well as several combinations of waves and current.

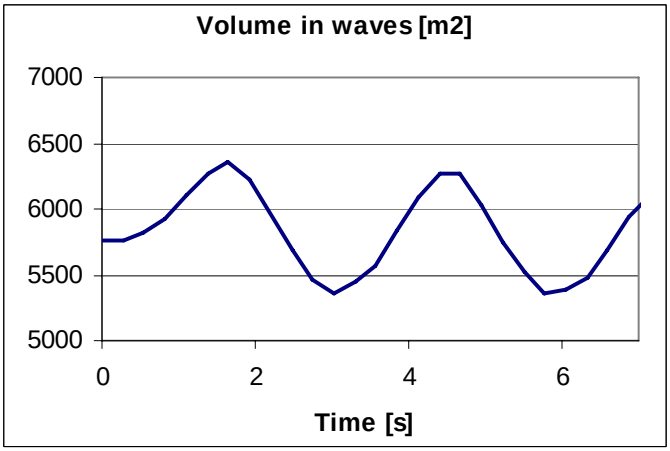

Figure 19 Net volume in waves. Wave height 3 m. Period 5.5 s.

Case study 3. Establishing operational design conditions

Much of fish escape in Norway is connected to net handling operations. Establishment of operational conditions to be considered with respect to both design criteria as well as criteria for operation procedures are included in the research project. The work has been divided to three stages.

1. Identification of potentially hazardous operations
2. Risk assessment, including simulation of action / response
3. Proposal for guidelines / rules

So far the work is at stage 1. The following operations have been identified:

Moving fish from one fish cage to another. In this operation cages are moved together, the two nets are joint. Fish are guided from one net to the other by reducing the volume of the original net, such that all fish has to enter the new net. Any mismatch or any accidents during this operation may lead to fish escaping.

Change of net while fish stays in cage. In this operation a new net is put into the cage between the floater and the net in use. Half the rims of the two nets are joint together, while the remaining two rims are attached on the floater as usual. The joint rims are lowered in the water so fish can swim between the two nets. The old net is then pulled up on the other side, released from the new net which is attached to the floater.

Installation of new net. As new nets are installed, contact with sharp objects must be avoided. This may lead to ripping of net causing holes where fish may escape.

Transport of nets. Ripping of the net material can also occur during transportation of the net from supplier to customer. These holes can cause fish escape.

Lifting of the net. In any case the net needs to be lifted for inspection or other purposes, holes in the net may be introduced. This may happen due to large local forces at lifting points. According to Moe and Krokstad (2004) the main origin for fish escapes from nets are ripping where the side and bottom part of the mesh connects. Moe and Krokstad (2004) show that the forces in the net during this operation are strongly dependent on the lift velocity.

Boat operations close to the cage. At any operation with boats close to the cage it is important to consider the net deformation. During strong sea current there is a hazard of direct contact between propeller and net.

Fish collection and sorting. During this process a separate net is used for collecting fish. At the latter stage of this process the remaining fish stock is collected simply by compressing the original net. There may be an uncertainty regarding the number of fish remaining in the net. This may lead to high fish mortality as fish are compressed. The operation may also introduce large forces in the net causing ripping and escape.

Installation and removal of weights. During this process the weights may introduce damage to the net as the weights are lifted/lowered between sea surface and the bottom of the net.

The above list form the basis for further phase 2 and 3 in the project, altough it may not be exthaustive. More operations may be added in case observed from further field studies.

CONCLUSIONS

Case studies on a typical polyethylene based fish farm for commercial use have been carried out and the following conclusions have been drawn:

Skew mooring system will increase the forces in the crowfoot mooring cables, and may increase the stress level in the floater even more. In the case presented forces in the crowfoot was doubled and the principal stress in the polyethylene was almost 3-doubled.

The volume reduction in current can be very large (almost 90% reduction seen in case studies), and is sensitive to both weights and current velocity. Also waves will reduce the volume and should be further investigated.

Several hazardous operations on fish farms have been identified and should be further considered in a risk assessment for overall importance.

ACKNOWLEDGMENTS

The work has been funded by Aquastructures, Hydrotech and the Norwegian research council, NFR. Their support is acknowledged.

REFERENCES

Altaposten(2004) “Vurderer mulkt etter laksedød” News article in Norwegian. http://www.altaposten.no/nyheter/article6785.ece.

Berstad, A. J., Tronstad, H., Ytterland, A. (2004)” Design Rules for Marine Fish Farms in Norway. Calculation of the Structural Response of such Flexible Structures to Verify Structural Integrity.”

D. Eberly, J. Lancaster, A. Alyassin, “On gray scale image measurements, II. Surface area and volume”, CVGIP: Graphical Models and Image Processing, vol. 53, no. 6, pp. 550-562, 1991.

Fredheim, A and O. F. Faltinsen (2003) “Hydroelastic analysis of a fishing net in steady inflow conditions”, Hydroelasticity in Marine Technology, Oxford, UK.

Fredriksson, D.W., M.R. Swift, J.D. Irish, I. Tsukrov and B. Celikkol, (2003). “Fish Cage and Mooring System Dynamics Using Physical and Numerical Models with Field Measurements.” Aquaculture Engineering, Vol. 27, No. 2, pp. 117-146.

Halse, K. H. (1997) “On Vortex Shedding and Prediction of Vortex-Induced Vibrations of Circular Cylinders.” Phd. Thesis. Department of Marine Structures, Faculty of Marine Technology, Norwegian University of Science and Technology (NTNU).

Lader, P. F., B. Enerhaug, A. Fredheim and J. Krokstad (2003) “Modelling of 3D Net Structures Exposed to Waves and Current”, Hydroelasticity in Marine Technology, Oxford, UK.

Lader, P. F. and B. Enerhaug. (1994) Experimental investigation of forces and geometry of a net cage in uniform flow. Accepted for publication in IEEE Journal of Ocean Engineering.

Løland, G. (1991) Current forces on and flow through fish farms. Phd Thesis. Department of Marine Hydrodynamics, , Faculty of Marine Technology, Norwegian University of Science and Technology (NTNU).

NAS(2003): “NS 9415 Marine fish farms – requirements for design, dimensjoning, production, installation and operation”. Publisher: Standards Norway, Pronorm AS Postboks 252, 1322 Lysaker, Norway. http://www.standard.no.

NMF (2003) “FOR 2003-08-12 nr 1052: “Forskrift om krav til teknisk standard for anlegg som nyttes i oppdrettsvirksomhet” (English: Regulation concerning requirements for the technical standard for installations which are used in fish farming activities) Norwegian Ministry of Fisheries. Postboks 8118 Dep, 0032 Oslo

Tronstad, H. (2000) “Nonlinear Hydroelastic Analysis and Design of Cable Net Structures Like Fishing Gear Based on the Finite Element Method” PHd thesis. Institute of Marine Technology NTNU, Trondheim.